ICAS-82-3.7.2

SLICED DISC DESIGN - A COMPOSITE CONFORM CONCEPT FOR A TURBO ENGINE AXIAL COMPRESSOR?

R.Kochendörfer

Institut für Bauweisen- und
Konstruktionsforschung
DFVLR - Stuttgart, W-Germany

Abstract

For an 800 kW turbo engine demonstrator an axial compressor concept in composite technology was developed. The aim was a reduction of mass and moment of inertia compared to a titanium design. The geometry and the blade spacing required a single-blade attachment concept. To minimize the problems in the shear loading area, the "compressor rotor" was divided into individual segments, made of aluminum alloy. Each of the Al-segments represents the root part of a B/Al blade. In the leading and trailing edge areas these segments are shrunk together by composite hoops, which also sustain the centrifugal loads. As long as the shrinkage pressure is present, the segmented disc exhibits a similar behaviour as an unsliced disc. This sliced disc concept was successfully proof-tested in cold spin tests up to the design level of 47600 rpm, corresponding to a maximum blade tip speed of 420 m/sec.

Introduction

Rotating structures like blades and discs are preferential applications for fiber reinforced composites. These structures are mainly loaded by centrifugal forces which lead to a predominant load path direction and allow consequently a high percentage of unidirectional fiber arrangement. Under these conditions the outstanding properties of advanced composites, i.e., high strength and high stiffness to density ratios in fiber direction, can be exploited with maximum benefit.

Due to a weight saving potential between 15% and 30% nearly every company in the field of turboengines is running programs to evaluate the applicability and reliability of composite engine components. From the design point of view most of these activities can be summarized as a substitution approach by replacing metal components like casings, blades or discs by composite parts.

Objective of investigation

The object of the investigations reported in this paper was a composite conform design approach for a three stage axial compressor rotor with fiber reinforced blades and discs. To increase rotor acceleration, a reduction of weight and moment of inertia, compared to a titanium design, was the main goal.

The design principles were to be proven by a hardware demonstration for the second stage rotor of an 800 kW-axial/radial gas generator. This contribution was part of a BMFT-sponsored research task "Advanced Compressor Components for Aircraft Engines" carried out in cooperation with the contractor, the German turbomachinery company MTU (Motoren- und Turbinen-Union, Munich) / 1 /.

Program tasks

The investigations can be classified into four sections:

- First, selecting the most favourable design approach out of a number of different rotor concepts.
- Second, verification and proof-testing of the rotor design principle, with emphasis on a low cost test program within a short time period.
- Third, blade design as well as fabrication and test of simplified blades, to gain realistic data for weight and cost predictions.
- Fourth, reference study on the basis of weight, moment of inertia and cost for the selected composite rotor design versus the reference titanium disc rotor and a projected titanium integral rotor.

Composite blade/disc concepts

The axial compressor geometry for the 800 kW turbo engine is shown in Fig.1. The flow path and the blade airfoil sections should be identical for the titanium version and for the composite design. Due to FOD-requirements only the second and third rotor stages should be replaced.

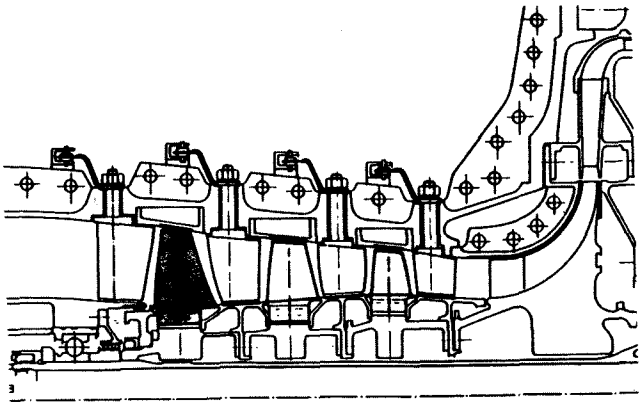

Fig. 1: Compressor geometry of the 8oo kW turbo engine

An integral blade/disc solution, Fig.2(a), was not feasible due to the center aperture requirement for the shafts. The geometrical conditions and the narrow blade spacing - 20 blades with 170 Ø mm tip diameter and 32° stacking angle - made a fiber conform loop attachment impracticable, Fig.2(b). This twin blade concept combines two blades by a parallel loop where the fibers are arranged continuously from one blade to the other / 2 /. The bi-loop wedge design, Fig. 2(c), with the fibers protruding straight out of the airfoil section being divided at the root end into two loops, is a fiber compatible single blade attachment. Because of the inherent stress level resulting from the small bending radius, this design approach can be realized successfully only by using small diameter fibers as reinforcement. The composite blades may be inserted individually into a suitably grooved disc in the same manner as their metal counterparts. However, in this particular application the bi-loop wedge blade concept could not be realized due to the attachment volume requirement. Fig.2(d),(e) show a single blade attachment, where the centrifugal forces of the blades are transfered to the root fittings by shear. The matrix controlled

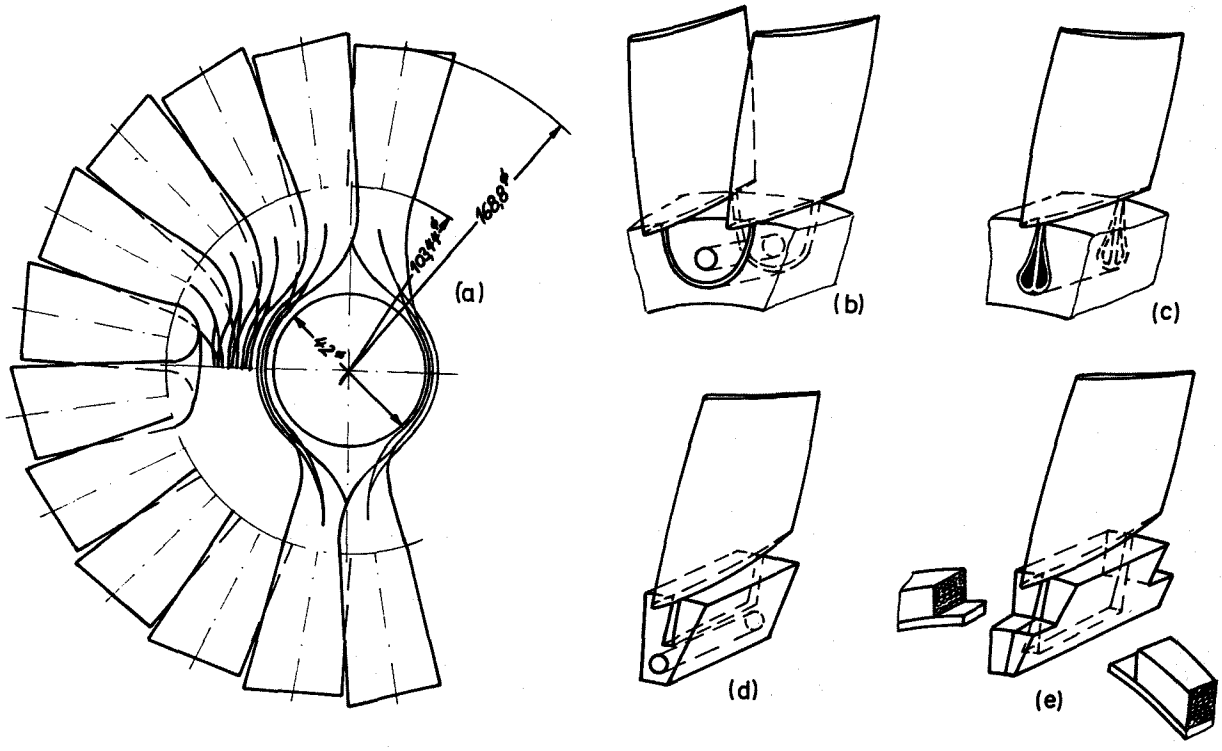

Fig. 2: Different composite blade/disc concepts
a) Integral blade/disc concept
b) Twin blade concept
c) Bi-loop wedge blade concept
d) Shear load attachment with bolt connection
e) Shear load attachment with composite hoops

shear transfer capability is a weak property for all composite materials, whereas the design approaches 2(a),(b),(c) are governed by the high fiber controlled properties of composite materials, e.g. high specific modulus in fiber direction. However, this shear loaded single blade attachment proved to be the only concept applicable.

Rotor design principle

To minimize the effects of low shear strength and high creep tendency at elevated temperature / 3 /, the load transfer area between the B/Al composite blade and the aluminum root fittings were maximized. The total area between blade platform and rotor shaft will be used as a shear transfer surface, Fig. 3,realized by a diffusion bonding process . The centrifugal load is carried by two composite rings below the leading and trailing edge areas, Fig. 4. Moreover, these composite rings shrink the aluminum blade roots into a compression stress state.
To realize a high compression prestrain level with the lowest possible composite ring tension prestrain, only certain parts of the aluminum blade roots are compression loaded. These contact surfaces between the individual blade roots are marked in Fig.5 as bright shining areas. To allow local deformation, slots are machined into the blade root to form "tongues".

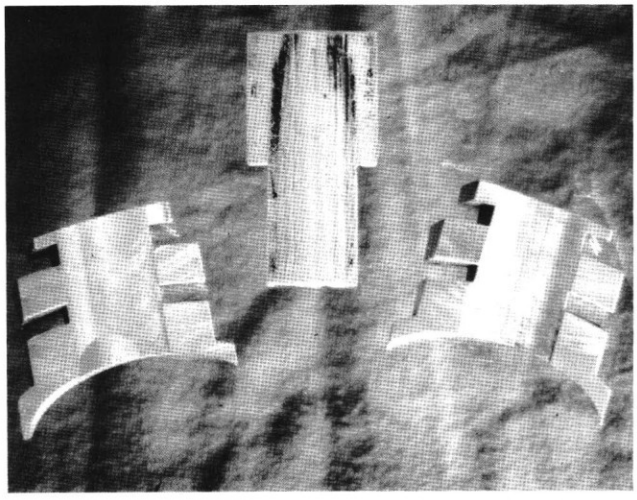

Fig. 3: Simplified B/Al blade and Al-root fittings

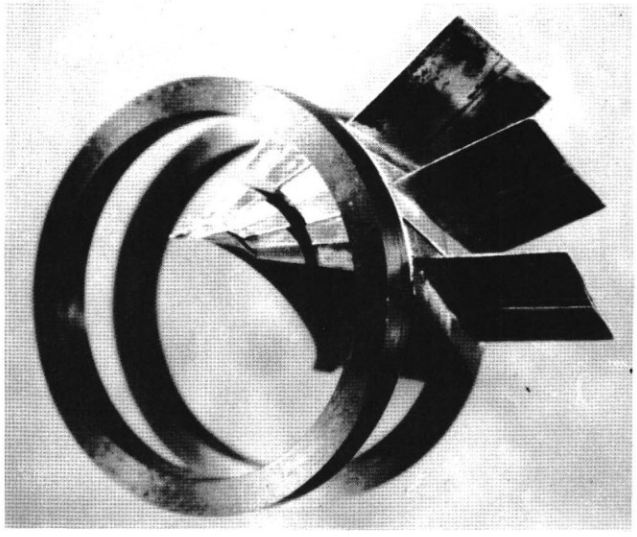

Fig. 4: Simplified B/Al-blades diffusion bonded to Al-blade roots, assembled into composite rings

With increasing speed the composite hoops will expand due to the centrifugal loads and the contact pressure between the individual blade roots will be reduced. The "sliced disc" shows a similar behaviour as the unsliced disc up to that speed where the composite ring elongation becomes equal to the prestrain level of the "Al-tongues".

Beyond that speed, gaps between the individual segments will appear. This event should occur at a high speed level corresponding to a high radial pressure between segments and hoops. This is expected to over-compensate for all distortions due to the gas flow or vibrations.

The centering of the disc and the torque transfer is realized by spacer tubes, Fig. 6. The spacers are mounted onto the composite rings with a certain shrinkage pressure, which essentially should remain positive over the total speed range. The shrinkage pressure has to be at least high enough to guarantee the torque transfer from rotor stage to rotor stage by friction.

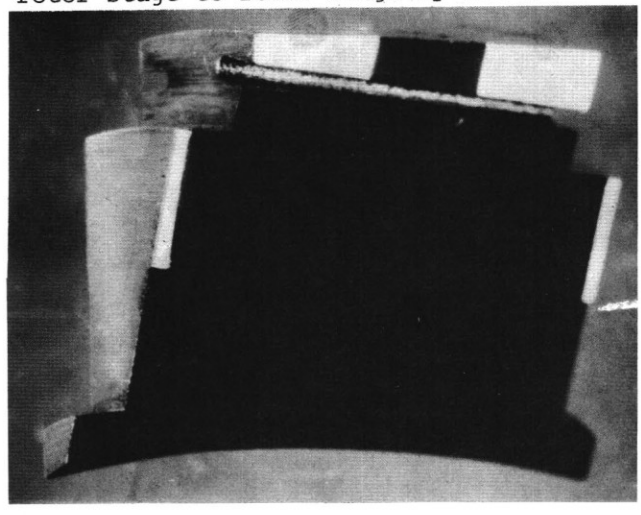

Fig. 5: Contact surfaces of the individual Al-blade roots and "tongues"

This shrinkage pressure p_d, Fig. 7, will be constant up to design speed if the centrifugal elongation of the spacer tube, due to its own weight is increasing equally with the composite ring elongation. This can be realized with composite spacer tubes by selecting a certain value of specific modules E/ϱ resulting from an appropriate fiber arrangement. Using titanium spacers the shrinkage pressure will slightly increase with increasing speed.

The calculated stresses versus angular frequency, Fig.7, show that the stress levels for the composite rings are within the design allowables up to design speed of 47600 rpm. This is valid for the circumferential stress σ_φ as well as for the radial stress σ_r. Fig. 7 also indicates that at about 25000 rpm gaps between the individual segments will occur. This event can not be shifted to a higher speed level, because the compression prestrain level of the aluminum "tongues" is mainly limited by plastic deformation.

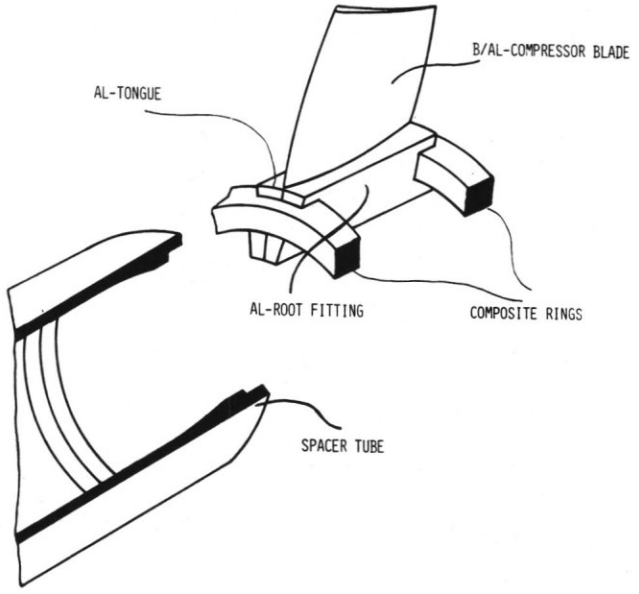

Fig. 6: Components for the "sliced disc" concept

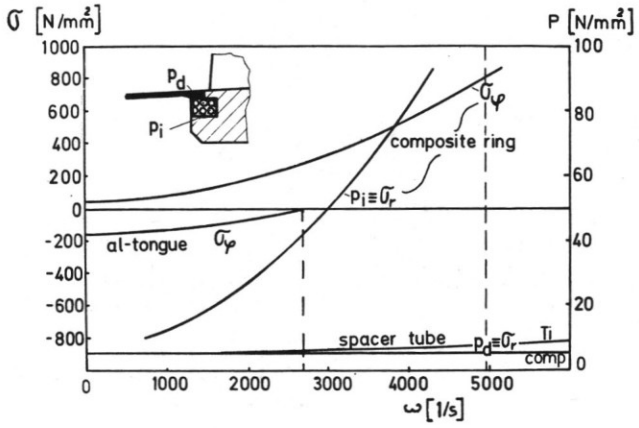

Fig. 7: Calculated stresses versus angular frequency

Interim balance

- The calculated stress level of the composite rings is well within design allowables
- Despite of the fact that a shear load type of attachment is not an optimum composite design solution, the shear stress level could be reduced to a subcritical value for B/Al material on the order of 15 N/mm²
- Up to about 25 000 rpm the "sliced-disc" exhibits a similar behaviour as an unsliced disc. At gap-opening-speed each individual segment is pressed against the hoops with a centrifugal force of 14 kN
- Only unidirectional fiber arrangement is realized, thus exploiting the composite potential with maximum benefit.

Despite these positive prospects, a number of questions arises for this sliced-disc-concept. To demonstrate the feasibility of the segmented rotor and to answer the main question concerning the stability or the unbalance tendency of the rotor, cold spin tests were conducted.

First test rotor

The first test rotor was fitted with two simplified B/Al blades. All other Al-segments had equivalent masses simulating the centrifugal force of the blades, Fig.8. Instead of a spacer tube, a metal coupling device was inserted into the rotor to take advantage of an already existing centrifuge spindle. This coupling device was slotted regularly and can thus be assumed as an additional internal pressure distribution.

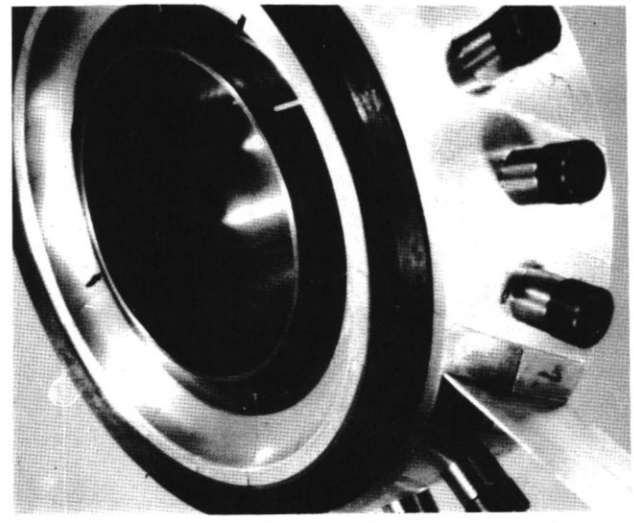

Fig. 8: First test rotor

The rotor offered a smooth run without any unbalance tendencies up to the burst speed of 32 000 rpm. This corresponds to a calculated burst speed of 40000 rpm without the coupling device, which will be replaced in the following tests and in reality by a spacer tube. But even then the burst speed was unexpectedly low. Neither a review of the rotor manufacturing procedures nor the composite ring fabrication data could give a complete explanation. The reconstructed failed rotor, Fig.9, gave a strong argument, that the composite ring located downstream failed first. A FEM-calculation verified this presumption, Fig.10. During the centrifugally tests the deformation of the aluminum segments changes the internal pressure distribution under the composite rings. This leads to a stress magnification factor of 1.7, corresponding to a composite ring local overstress at the inside ring corners.

As a consequence of the failure evaluations and of the effects observed during the first rotor test, a number of modifications was made. The most essential redesign step was the improvement of the load transfer from the segments into the composite rings by milling a clearance into the aluminum segment contact surface, with a progressive-increasing thickness according to the segment deformation characteristics. At zero speed only the outward section of the segments are in contact with the hoop. With increasing speed the contacting surface increases corresponding to the segment deformation. At design speed the entire segment surface is coupled to the ring with an almost constant pressure distribution. By this means critical radial stress peaks, as well as critical shear stress peaks, within the composite rings can be avoided.

Two essential decisions should be mentioned:

First, to proof-test the composite rings before rotor assembly to ensure the quality of that tension loaded member within the rotor components which guarantees the rotor reliability.

Second, to measure the rotor during the cold spin test procedure very carefully between the stepwise increasing speeds.

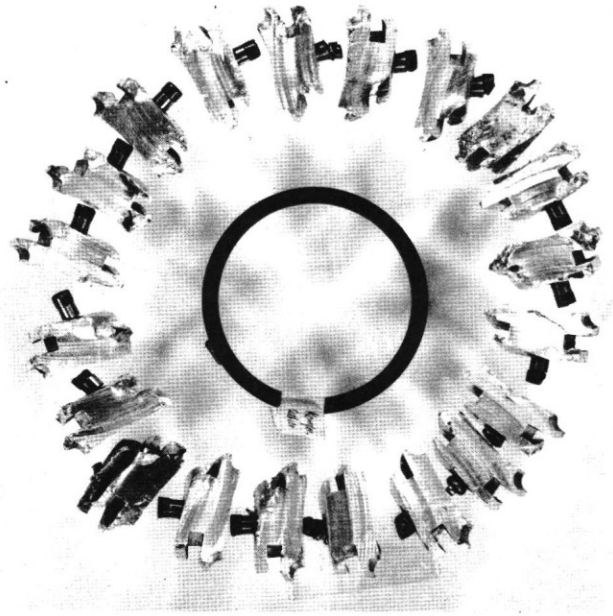

Fig. 9: Reconstruction of the failed first test rotor

Composite ring qualification

The composite rings should be proof-tested under almost the same loading conditions as in the real case. It would be advantageous if the testing device offers not only the necessary reproducibility but also a multiple utilization.

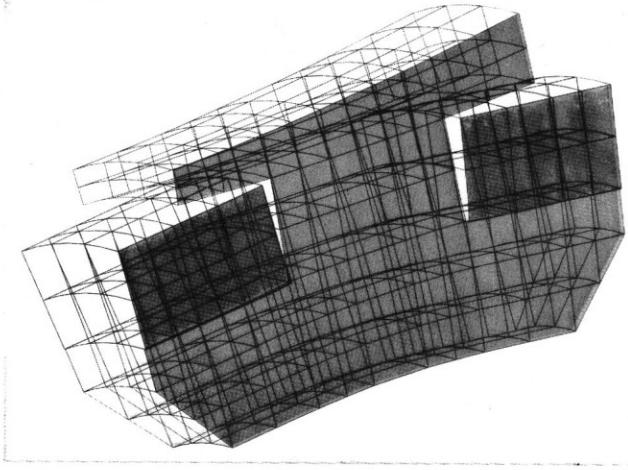

Fig. 10: Finite element calculation for the first test rotor

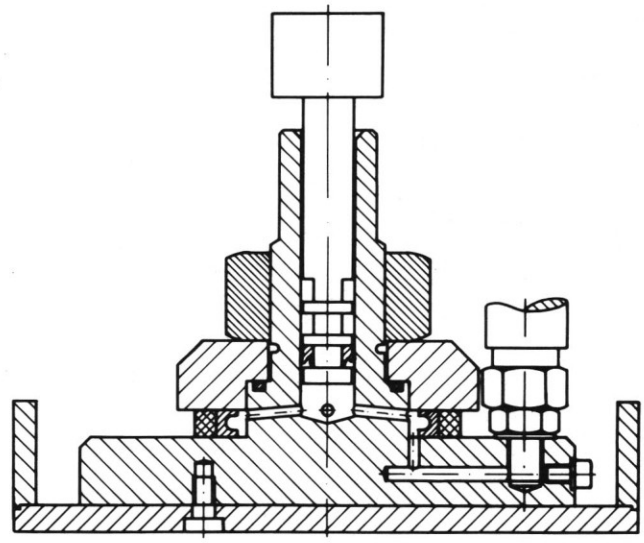

Fig. 11: Internal pressure device for ring qualification

With a specially designed internal pressure device, Fig.11, sealing problems arose at oil pressures beyond 1200 atm. According to Fig.7 this internal pressure is adequate to test the hoop up to design speed stress levels, but is not sufficiently high to load the rings up to failure.

Thus, cold spin tests remained the only possibility to realize high test ring stresses / 4 /. To achieve this high stress level at moderate test speeds, an additional internal pressure load was necessary.

Fig. 12: Cold spin test device for ring qualification

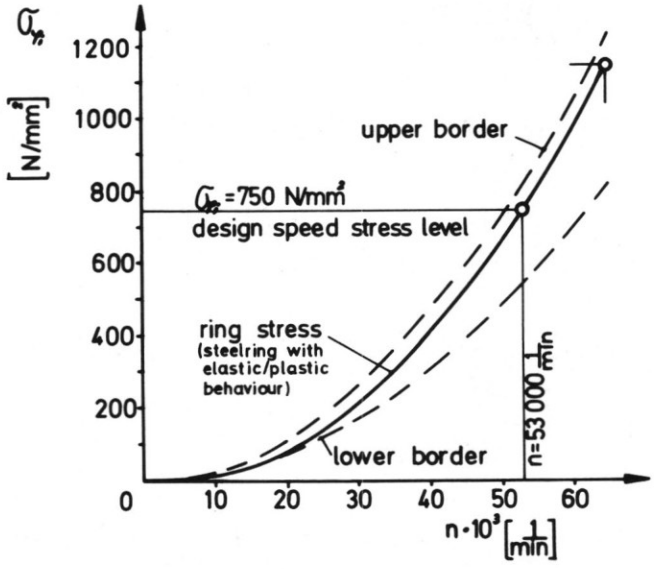

Fig. 13: Stress calculation for composite ring spin tests

For this purpose a regularly slotted metal disc was inserted into the test ring, analogous to the coupling device of the first test rotor, Fig. 12. To equalize the stress distribution, a closed metal ring was arranged between the metal disc and the test ring. This metal ring will be strained up to a plastic deformation with increasing speed, a fact which has to be considered in the stress calculation, Fig.13. The upper borderline is gained by assuming the steel ring to be unstressed and acts only as an additional mass. For the lower borderline, the assumption is made that the stressed steel ring offers a pure elastic behaviour which could not be realized in this particular case even with a high strength steel. The calculated composite ring stress is close to reality and takes into consideration the elastic/plastic deformation according to a measured stress/strain curve of the particular steel ring material. The composite rings for the test rotors were qualified up to the design speed stress level. Two additional rings, fabricated within the same batch, were tested close to failure stress (according to the rule of mixture) offering a safety margin of 1.5 .

Second test rotor

For ease of fabrication, balancing, measuring and testing the redesigned second test rotor had no blading, Fig. 14. Dummies were simulating the blade centrifugal loads. Metal spacer tubes act as a centering and torque transfer device similar to a later rotor application. The second test rotor was spin-tested up to the design speed of 47 600 rpm without any problem. During all the tests it never became necessary to balance the rotor again.

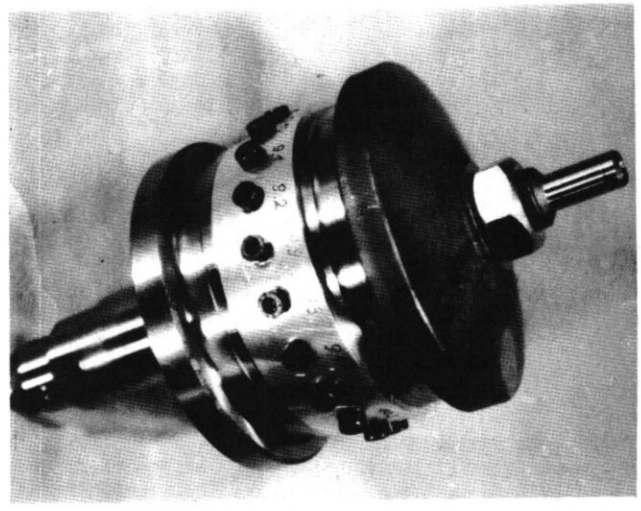

Fig. 14: Second test rotor after successful cold spin test to 47 600 rpm

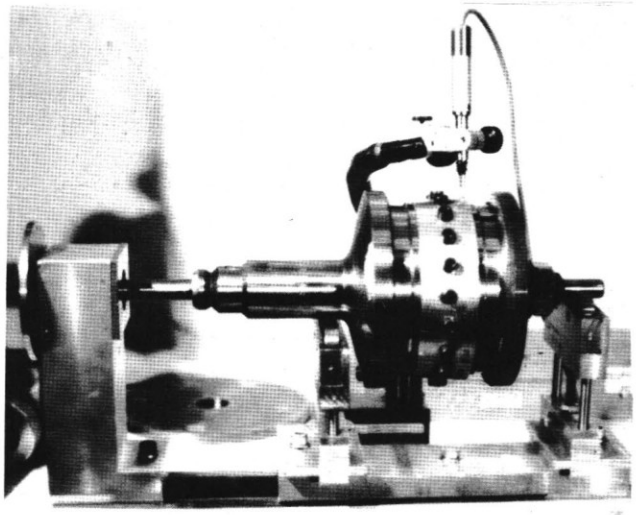

Fig. 15: Device to measure the rotor geometry

Information concerning the opening and closing mechanism of the individual segments were gained by carefully measuring the rotor geometry step by step with increasing speed, Fig.15. The results can be summarized as follows:

(1) The individual segments moved relatively to each other in radial direction - but less than 30 µm.
These effects can be explained by a release of internal stresses, originating from the rotor assembly procedure.
From these displacements no measurable change of rotor balance was observed.

(2) As predicted by the analytical evaluation, gaps between the individual segments seem to have appeared between 30 000 rpm and 35 000 rpm. This can be deduced from the measured segment displacements, because:

(3) Beyond this gap-opening-speed, no relative motion of the individual segments was noticed, e. g., the segment arrangement relative to each other was constant over more than 50 spin test cycles.

After that stable period, a relative motion of the segments was noticeable again, coinciding with an enlargement of the rotor diameter and followed by a rotor failure at 45 000 rpm. This can be explained by the crack growth within the aluminum segments, a thesis, which is proved to be true by reconstructing the burst second test rotor, Fig. 16. Obviously, a number of aluminum segments failed, before the composite rings were overstressed.

Fig. 16: Reconstruction of the failed second test rotor

Rotor test balance

The results gained with these two test rotors were very encouraging.

- The main question concerning the stable behaviour of the sliced rotor has been answered. The first and the second test rotor showed no unbalance tendency.
- A reproduceable motion of the individual rotor segments could be proof-tested with the second rotor. As a consequence of these tests, the recommendation can be made to spin test a real rotor beyond gap-opening-speed, before final machining. The effects of vibrations and aerodynamic blade loads could not be tested in these cold spin tests. However, at gap-opening-speed the segment contact pressure at the hoops is quite high. Thus, it may be assumed that the clamping condition will be similar to that of usual dovetail metal blades.
- The centering function of the spacer tube could be successfully proof-tested. Torque transfer occured only during the accelerating and decelerating test phase. No problems were noticed concerning the spacer tubes.
- Only small changes in rotor design seem to be necessary to pass the low cycle fatigue tests.

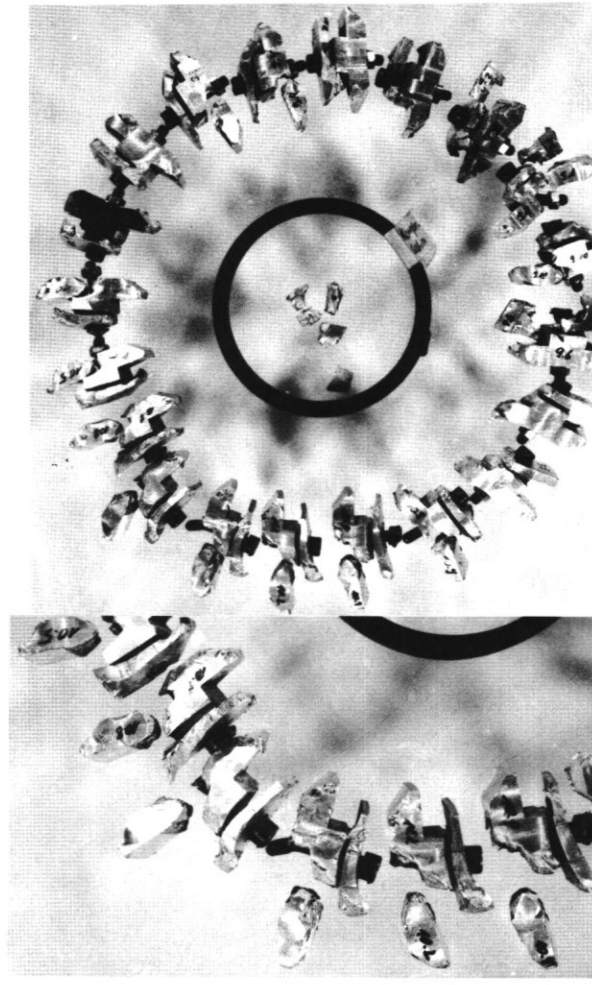

B/Al-blading

Within this program the main activity was concentrated on evaluating the feasibility of the sliced-disc-rotor concept. Concerning the blade fabrication, only selected investigations were made, mainly concerning the small blade size effects. This was possible due to a background of a 10-year's experience in B/Al processing technique and the experience gained with the previous program, where a B/Al-J 79 first stage compressor blade was realized and tested / 2 /.

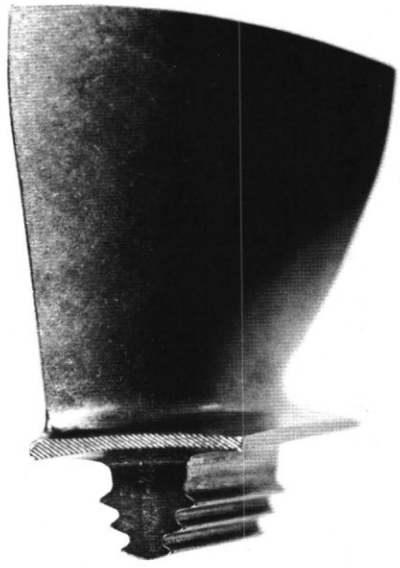

Fig. 17: Titanium-compressor blade for the second rotor stage

	0° B/Al	0° CFRP	Ti6Al4V
$E_{\parallel}$ [KN/mm²]	210	200	110
$E_{\perp}$ [KN/mm²]	100	8	110
$\sigma_{\parallel}$ [N/mm²]	1000	850	1000
$\sigma_{\perp}$ [N/mm²]	130	35	1000
G [KN/mm²]	46	6	44
$\alpha_{\parallel}$ [10^{-6}/°C]	5.7	-1	8.5
ρ [g/cm³]	2.7	1.5	4.45

Fig. 18 Design data for different materials

The blade dimensions of the axial compressor for a 800 kW turbo engine represent the lower limit for a composite application. The compressor blade of the second stage rotor, Fig.17, had a length of 30 mm, a maximum airfoil thickness of 2.8 mm and edge radii of less than 0.15 mm.

As indicated in Fig.18, B/Al material is a more favourable candidate to replace titanium blades than CFRP. Moreover, B/Al offers a temperature stability, Fig.19, and an erosion- and impact resistance superior to that of CFRP.

Fig.20 shows the results of sand erosion tests; the eroded depth of a simplified airfoil section with an edge radius of 0.15 mm is plotted versus impacting time. Obviously, the aerodynamic efficiency of a CFRP-airfoil decreases earlier and faster than a B/Al-airfoil.

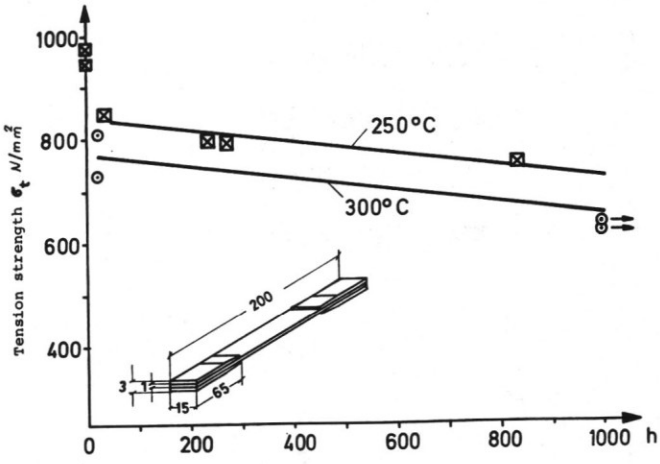

Fig. 19: Stress rupture properties for unidirectional B/Al (BB_4C/6061)

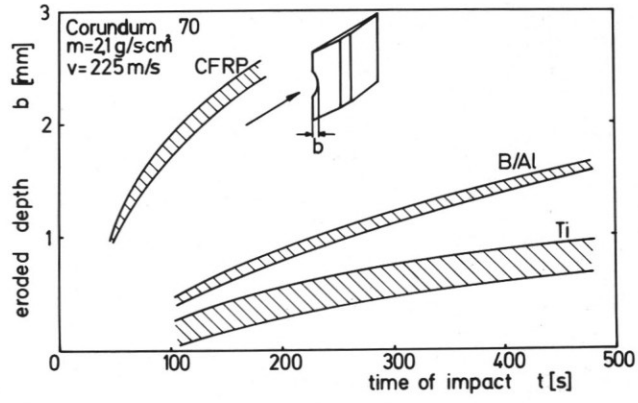

Fig. 20: Sand erosion tests with simplified air foil sections

With filament-foil-material, Fig.21, higher values of impact resistance could be obtained than by using prefabricated plasma spray material. Despite a large number of parametric studies / 5 /, (changing the processing parameters -time, temperature, pressure, atmosphere -, the fiber type and the matrix materials) it proved to be impossible to realize high impact resistance combined with high shear strength, Fig.22.

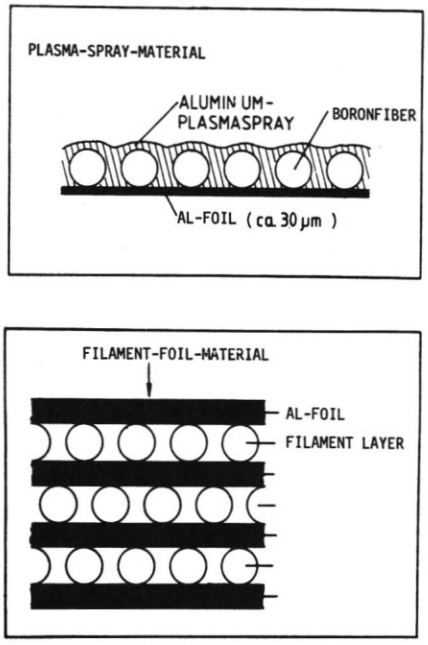

Fig. 21: Different types of prefabricated B/Al materials

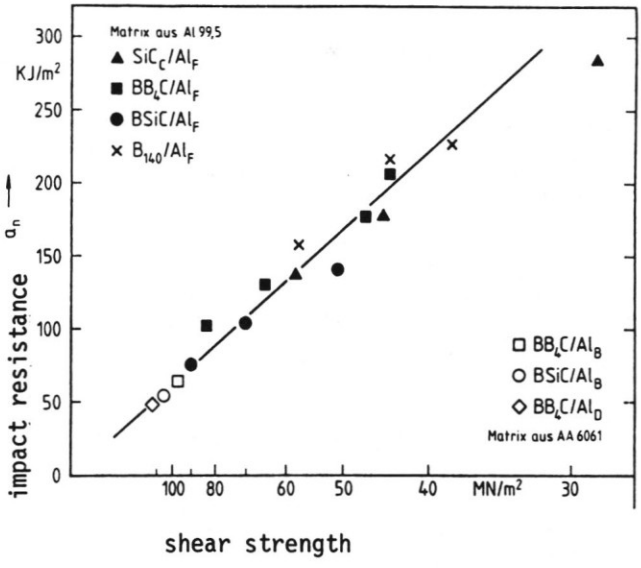

14o$^{\phi}$ µm-fibers; $v_f \sim$ 47%

Fig. 22: Impact resistance versus shear strength

High impact resistance is essential to fulfill the foreign object damage requirements. A high shear strength corresponds to a good fiber/matrix and matrix/matrix bonding which is a premise for an excellent dynamic behaviour.

The blade design is a core/shell concept. A unidirectional reinforced B/Al core carries the centrifugal loads and guarantees a low thermal elongation. Torsional stiffness and edgewise bending stiffness is increased by a non-reinforced 50 µm thick steel lamina, which also improves erosion resistance and impact behaviour.

The blade manufacturing technique already takes into account the aspects of serial production and quality assurance. The fabrication steps can be defined as follows:

- Prefabrication of single layer filament-foil products
- Cutting the single layer contour
- Precompacting the package of all single layers
- Twisting the precompacted package
- Steel skin brazing and material consolidation to the desired airfoil contour
- Brazing the B/Al/St-airfoil to the aluminum root fittings.

To check this manufacturing technology and to evaluate realistic production cost, a fabrication device was constructed with two pressing stages and a pneumatically controlled handling and transportation unit, Fig.23.

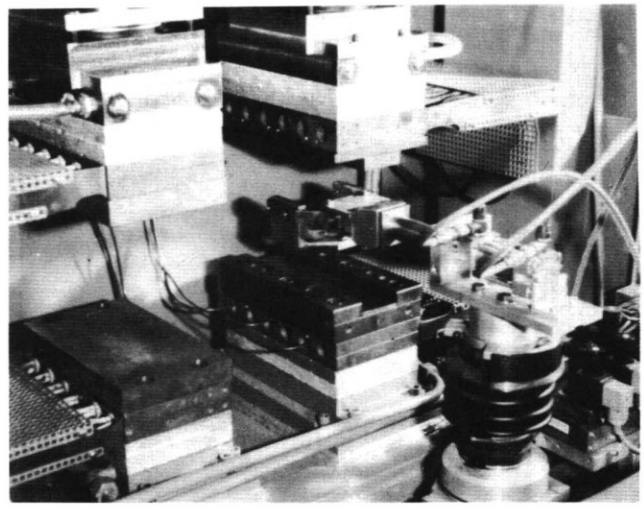

Fig. 23: B/Al-blade fabrication equipment

Simplified untwisted B/Al-blades with and without a steel skin, see Fig.3 and 4, were produced using this equipment and tested on an electrodynamic vibrator in fundamental flapwise bending mode.

The results showed, that for B/Al blades, a dynamic behaviour similar to that of adequately tested titanium blades was reached at the first attempt.

Potential of the sliced-disc-design

Due to testing requirements, the basic rotor concept was a titanium disc approach with inserted single titanium blades. This disc/blade design is rig-tested in a 3-axial/1-radial compressor configuration. The light weight design counterpart is a titanium integral rotor, which is in a design phase at the moment. Based on the second stage rotor the values for mass and moment of inertia are listed in Fig. 24 for both design approaches. Comparable to these figures, the corresponding values for the sliced-disc-concept in the state of a redesigned second test rotor are also shown. Compared to the titanium rotor with inserted titanium blades, the sliced-disc-rotor with B/Al blades (covered with a 5o µm steel foil) will offer a mass reduction of almost 5o% and a reduction in moment of inertia of 4o%.

These values are only slightly above the values for an integral titanium rotor, especially for the moment of inertia.

The cost for a titanium integral rotor and a sliced-disc-rotor can be assumed to be equal at a first glimpse. However, the reject probability and especially the reject cost will be higher for the titanium integral rotor.

Moreover, the danger of a blade loss due to fatigue failure is almost negligible for a B/Al bladed sliced-disc-rotor, whereas this will be the most probable failure mode for the titanium integral rotor.

Additionally, compared to a titanium integral rotor, the containment problems will be less pronounced for the sliced-disc-rotor.

	Sliced disc rotor	Titanium disc rotor	Titanium integral rotor
m [kg]	o,655	1,224	o,512
Θ [m^2kg]	$1{,}47.1o^{-3}$	$2{,}43.1o^{-3}$	$1{,}4.1o^{-3}$
Cost [DM]	~ 13ooo	-	~ 15ooo

Fig. 24 Mass, moment of inertia and cost for different rotor concepts

Summary

The design principle of a sliced-disc-rotor was successfully proof-tested in cold spin tests.

There are still questions left concerning the rotor dynamics of a multi-stage-rotor and the rotor behaviour under real engine operating conditions. However, the reductions in mass and moment of inertia are substantial compared to a titanium disc rotor with inserted titanium blades. It even seems to be realistic to design a B/Al bladed sliced-disc-rotor with the same moment of inertia as a titanium integral rotor but with a smaller rotor enlargement under centrifugal loads.

Due to the fact that the sliced-disc-design is not restricted by rotor size, it would be worthwhile to study the feasibility of this light-weight design concept for all those applications, where an integral titanium rotor design could not be verified up to now.

References

(1) Weiler W., Neue Technologien für Verdichter von Luftfahrttriebwerken, 2. BMFT Statusseminar Luftfahrtforschung und Luftfahrttechnologie, Garmisch, Oct. 198o

(2) Kochendörfer R., A New Type of Attachment for B/Al Compressor Blades, 1oth ICAS-Congress, Ottawa, Oct. 1976

(3) Melnyk P., Toth I.J., Development of Impact Resistant B/Al Composites for Turbojet Engine Fan Blades, NASA CR 13477o, May 1975

(4) Kochendörfer R., Compression Loaded Ceramic Turbine Rotor, 49th AGARD Meeting, Cologne, Oct. 1979

(5) Jacobsen G., Studie zur Verstärkung von Aluminium mit Bor- und Siliciumcarbid-Fasern, Dissertation Universität Karlsruhe, Mai 198o

Acknowledgements

The autor would like to acknowledge the help received from the colleagues of the Institut für Bauweisen- und Konstruktionsforschung with special reference to Mr. Dollhopf, Mr. Dudenhausen, Mr. Georgi and Mr. Vogler